ADVANCED MATERIALS TECHNOLOGIES

Supporting Information

for *Adv. Mater. Technol.*, DOI 10.1002/admt.202301288

Fully Inkjet-Printed, 2D Materials-Based Field-Effect Transistor for Water Sensing

*Xiaoyu Sui, Sonal V. Rangnekar, Jaesung Lee, Stephanie E. Liu, Julia R. Downing, Lindsay E. Chaney, Xiaodong Yan, Hyun-June Jang, Haihui Pu, Xiaoao Shi, Shiyu Zhou, Mark C. Hersam and Junhong Chen**

Supporting Information

Fully Inkjet-Printed, 2D Materials-Based Field-Effect Transistor for Water Sensing

Xiaoyu Sui, Sonal V. Rangnekar, Jaesung Lee, Stephanie E. Liu, Julia R. Downing, Lindsay E. Chaney, Xiaodong Yan, Hyun-June Jang, Haihui Pu, Xiaoao Shi, Shiyu Zhou, Mark C. Hersam, Junhong Chen*

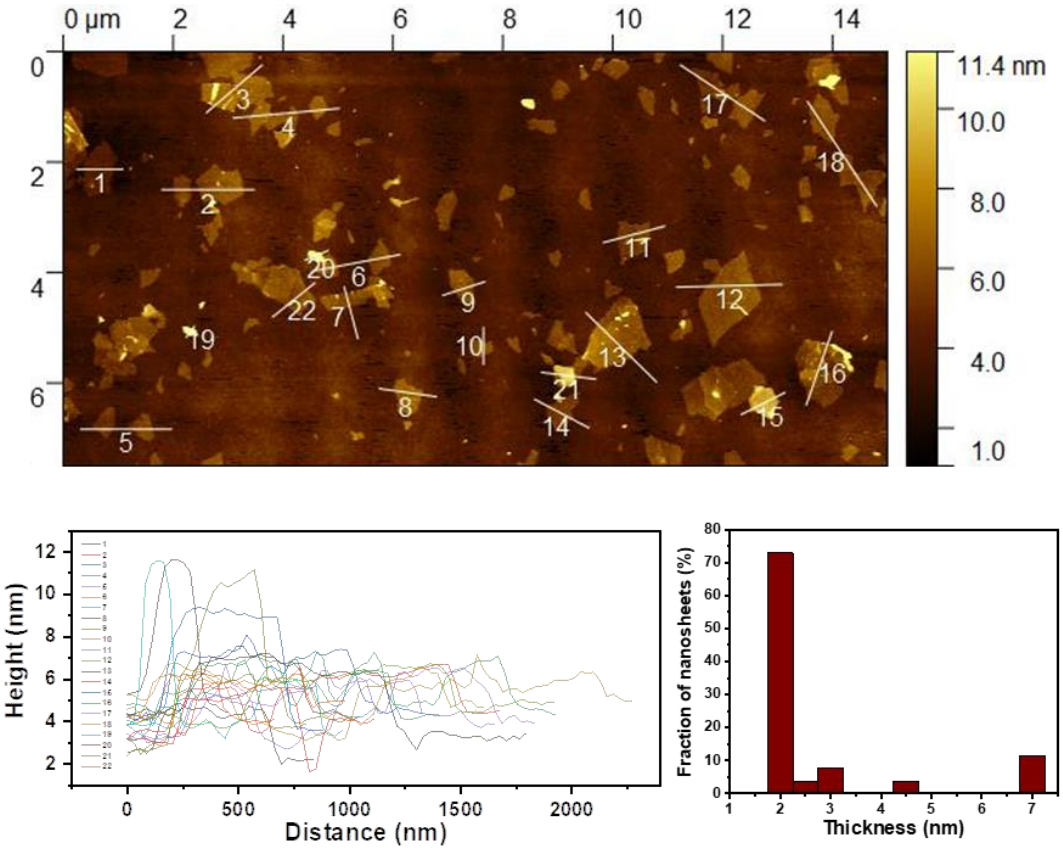

Figure S1. AFM image and line-scan profiles of MoS_2 nanosheets.

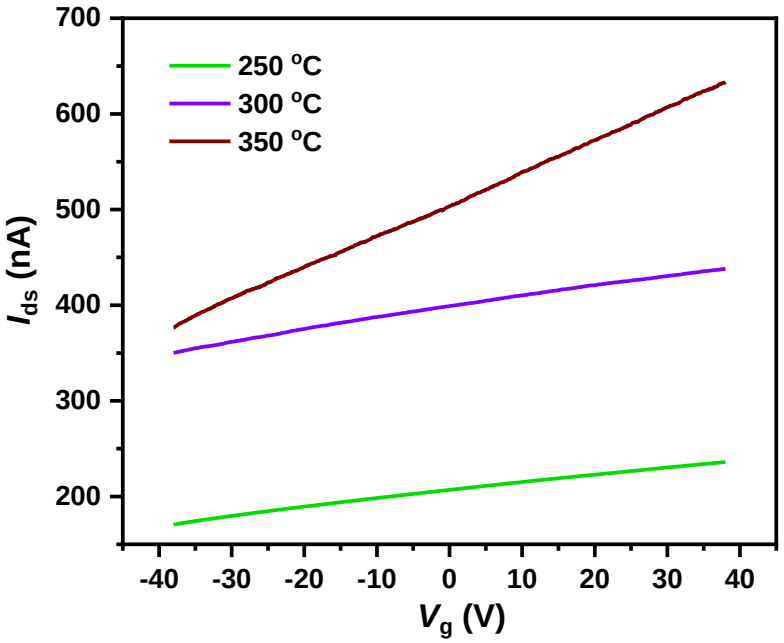

Figure S2. Typical transfer curves of MoS_2 parallel line patterns with six printing passes after annealing at different temperatures.

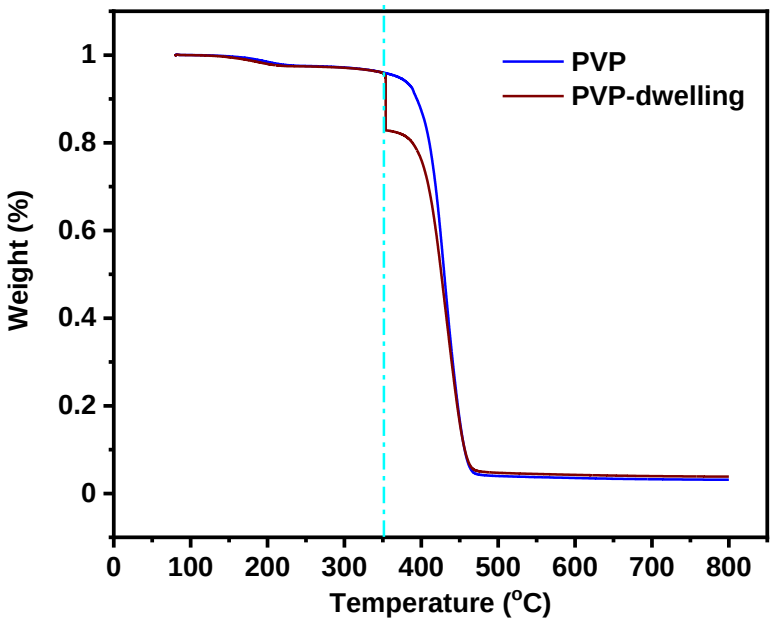

Figure S3. TGA of polyvinylpyrrolidone (PVP) with (wine) and without (blue) 1 h dwell time at 350 ^{o}C during the heating process.

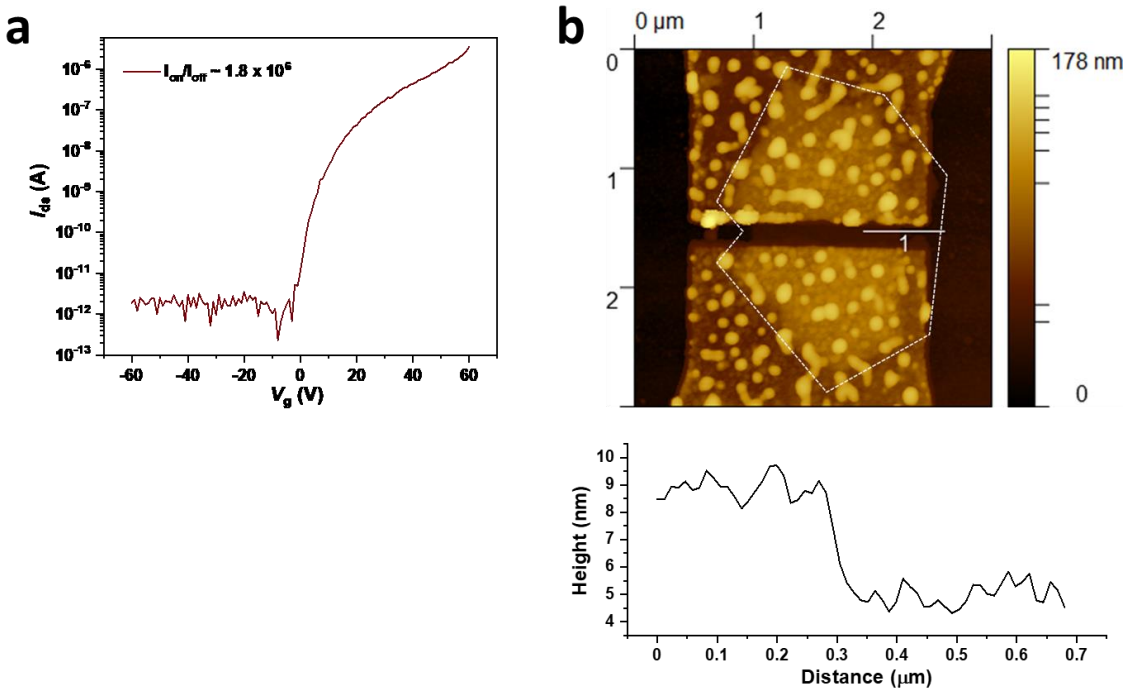

Figure S4. a) A typical transfer curve of a single-nanosheet device fabricated on a 300-nm-thick SiO_2/Si substrate with V_{sd} = 1 V. b) AFM image of a single-nanosheet device with a line-scan profile. Dashed outline indicates the MoS_2 nanosheet beneath the gold electrodes.

Mathematical Modeling Work Discussion

Mathematical modeling efforts were made to develop a spaced parallel printing strategy (i.e., print parallel lines abreast with overlaps) to achieve a wider, thin channel having a stable percolation network. The optimal drop spacing d and the number of printed parallel lines n need to be identified.

Let X denotes an average single printing pass cross-sectional profile and $X(w)$ denotes the X value at crosswise location $w \in [0, W]$ where W is the width of a single pass line. Note that $X(w) \geq 0$ at $w \in [0, W]$ and $X(w) = 0$ in $w \notin [0, W]$. In our analysis, $W = 70\ \mu m$.

When we overlap multiple parallel lines spaced by $d\ \mu m$, the resulting channel will be thicker in the center and thinner toward each side, i.e., two edges, because there will be more overlaps of printed lines in the center. Our goal is to make the center part have a relatively flat surface with average heights close to T, where we select $T = 1$, aiming to have an average single layer coverage at the center. To achieve this goal, we formulate an optimization problem:

$$\min_{n,d} \quad \sum_{x=L}^{U} \left\{ \sum_{k=0}^{n-1} X(x - kd) - T \right\}^2 \tag{1}$$

$$s.t. \qquad d > 5\ \mu m \tag{2}$$

$$L = \left\lfloor \frac{\{W + (n-1)d - C\}}{2} \right\rfloor \tag{3}$$

$$U = \left\lceil \frac{\{W + (n-1)d + C\}}{2} \right\rceil \tag{4}$$

where $[L, U]$ is the "center part of the channel that we are interested" (called *the center part*, hereafter) where L and U denote the lower and upper crosswise locations of the center part, respectively. Because the inkjet printer we use can only space lines by $\geq 5\ \mu m$, a constraint $d \geq 5\ \mu m$ is set in (2). Notice that the width of the resulting channel will be $W + (n-1)d$. By defining the width of the center part, denoted by C, we can determine L and U as shown in (3) and (4). We use $C = 70$ for our analysis. With the given constraints, we find the optimal n and d that minimize the pixel-wise sum of the square root of errors within the center part where the error is defined by the difference between the thickness of the resulting channel profile and T as shown in (1). We find the optimal solutions by grid search. Figure S5 shows the optimal average cross-sectional thickness profile of the resulting channel where the optimal line number is $n^* = 27$, and the optimal distance is $d^* = 5\ \mu m$.

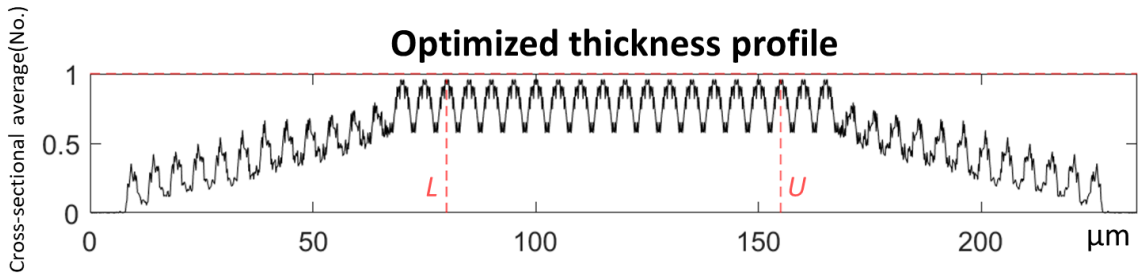

Figure S5. The optimized average thickness profile of the MoS_2 channel with $n^* = 27$ single pass parallel lines (i.e., Figure 3a) abreast, spaced by $d^* = 5\ \mu m$. The center part of our interest is between two vertical dashed lines, each of which represents L and U, respectively. We used $C = 70$. The horizontal dashed red line represents $T = 1$.

Unfortunately, the optimum channel could not achieve the highest thickness level larger than 1 upon the current ink formulation. Because the constraint of printing lines at least with a minimum 5 μm distance apart does not lead to thick enough printed channel. There are two approaches to address this problem: First, one may formulate thicker ink, e.g., higher concentration. Second, as a more feasible and general way to deal with the given ink formula, one may print twice for each line, i.e., 2 printing passes to make the baseline profile thicker as shown in Figure S6a. The resulting average thickness profile of the optimal channel is shown in Figure S6b (same to Figure 3c) where the optimal parallel line number is $n^* = 18$ and the optimal distance is $d^* = 7.19\,\mu m$. The center region is relatively flat and wide with a thickness of 1.52 at multiple peaks, thicker than 1 layer deposition, which ensures a stable percolation network. One can lengthen the center region arbitrarily by increasing C to make a wider percolation network. For example, Figure S6c shows the optimized channel with increased $C = 100$ where $n^* = 22$, and $d^* = 7.19\,\mu m$. Notice that only the center part is lengthened; it indicates that we can establish a more robust percolating network by lengthening the center region without changing the network thickness.

Our modeling work exhibits a spaced parallel printing approach to address the ubiquitous coffee-ring effect during printing fabrication, promising a uniform and robust 2D flake percolation network in the center of the printed channel.

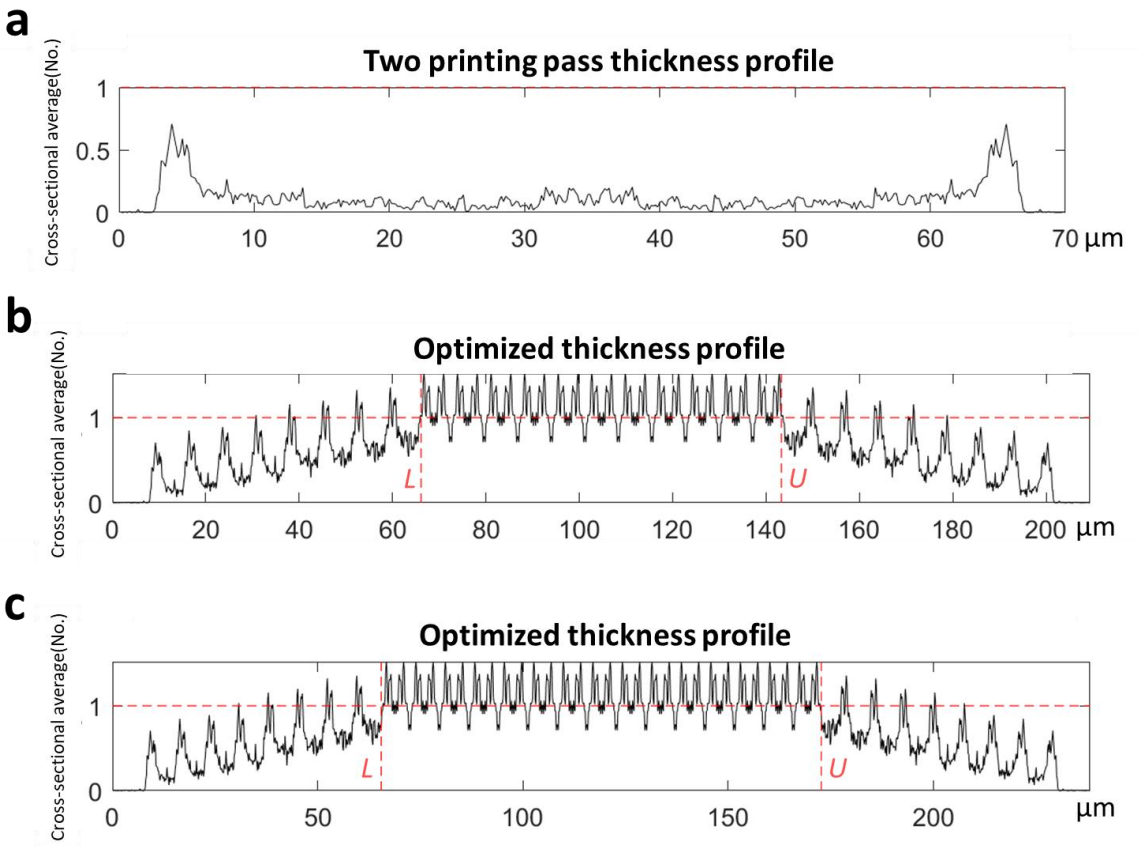

Figure S6. a) Average cross-sectional thickness profile from two printing passes. b) The optimized average thickness profile of the MoS_2 channel with $C = 70$, $n^* = 18$ two printing pass parallel lines (i.e., Figure S6a) abreast, spaced by $d^* = 7.19\,\mu m$. c) The optimized average thickness profile of the MoS_2 channel, which is achieved with C = 100, $n^* = 22$ two printing pass parallel lines (i.e., Figure S6a) abreast, spaced by $d^* = 7.19\,\mu m$. The center part of our interest is between two vertical dashed lines, each of which represents L and U, respectively. The horizontal dashed red line represents $T = 1$.

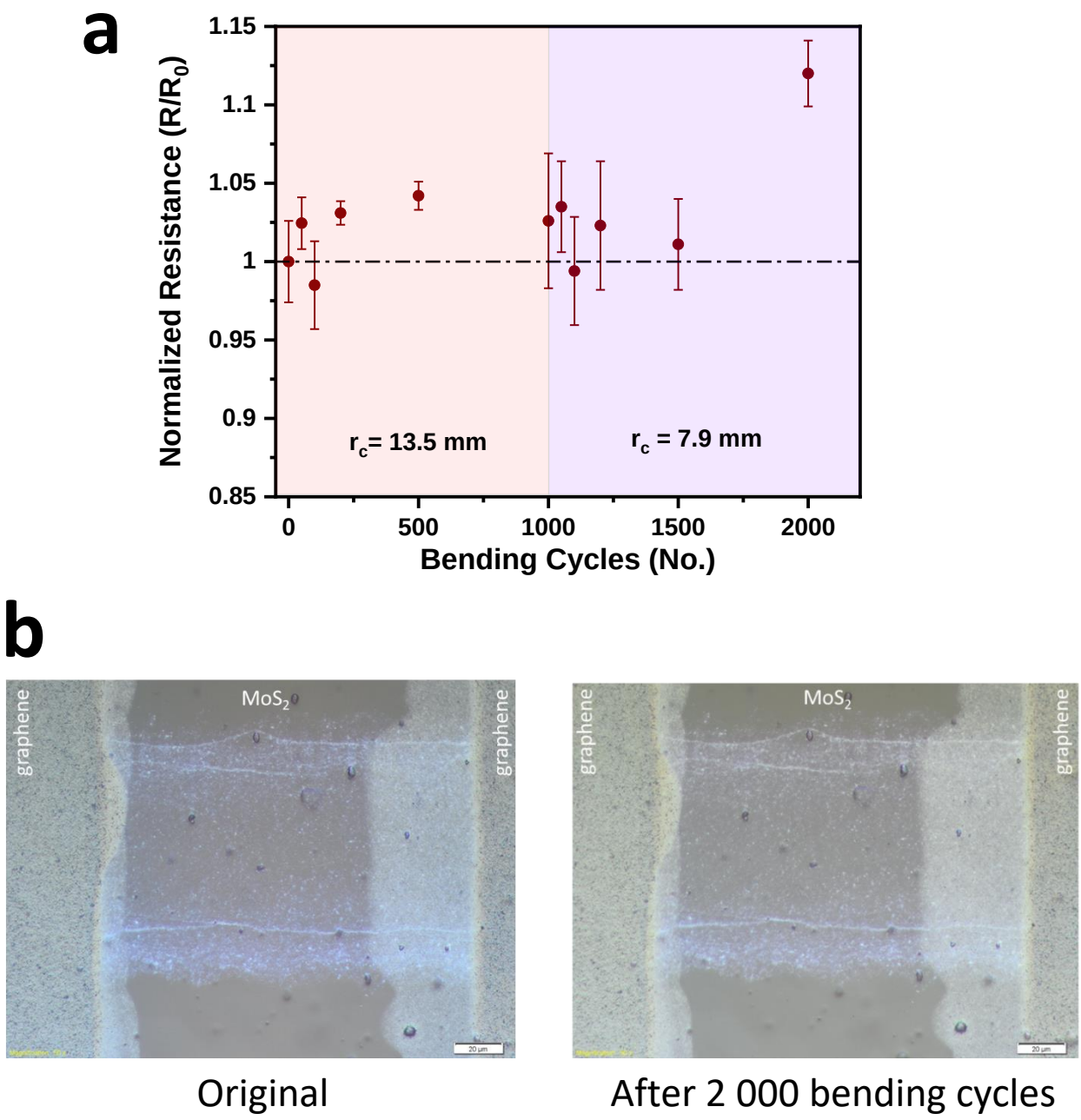

Figure S7. a) Normalized resistance of printed water sensors on polyimide over 2 000 bending cycles along the channel length. b) Optical images of the device before and after bending tests.

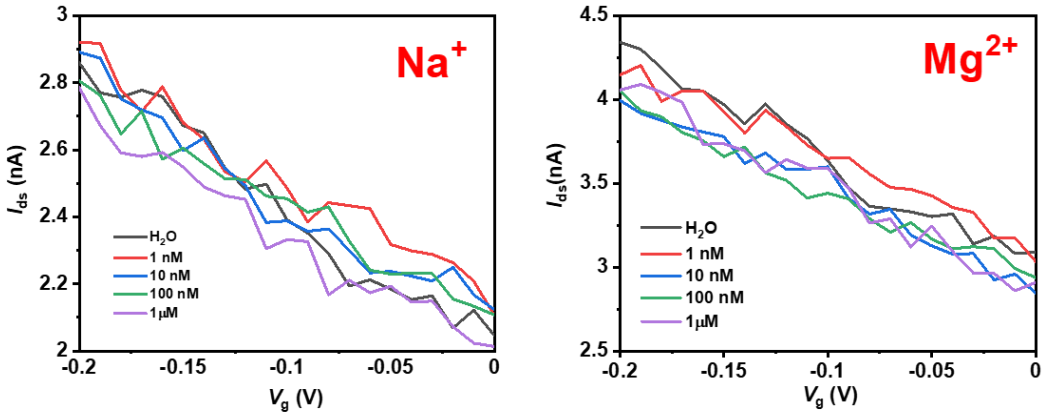

Figure S8. Water sensor responses to a) Na^+ and b) Mg^{2+} in water.

Table S1. Performance comparison of inkjet-printed MoS_2 semiconducting channels onto oxide substrates

Materials	On-Off ratio	Mobility ($cm^2\ V^{-1}\ S^{-1}$)	Channel length (μm)	Printed electrodes	Device application	Reference
MoS_2	~3,000	> 0.27	400	Yes graphene	Water sensor	This work
MoS_2	~200	4	~100	Yes graphene	None	1
MoS_2	6,500	0.02	140	Yes graphene	None	2
MoS_2	~50	0.06 ± 0.02	~0.1	No electron-beam lithography	Digital integrated circuits	3
MoS_2	2	-----	< 250	Yes silver	Photodetector	4

References

[1] J. Kim, D. Rhee, O. Song, M. Kim, Y. H. Kwon, D. U. Lim, I. S. Kim, V. Mazanek, L. Valdman, Z. Sofer, J. H. Cho, J. Kang, *Adv. Mater.* **2022**, 34, e2106110.

[2] O. Song, D. Rhee, J. Kim, Y. Jeon, V. Mazanek, A. Soll, Y. A. Kwon, J. H. Cho, Y. H. Kim, J. Kang, Z. Sofer, *Npj 2d Mater Appl* **2022**, 6.

[3] T. Carey, A. Arbab, L. Anzi, H. Bristow, F. Hui, S. Bohm, G. Wyatt-Moon, A. Flewitt, A. Wadsworth, N. Gasparini, J. M. Kim, M. R. Lanza, I. McCulloch, R. Sordan, F. Torrisi, *Adv. Electron. Mater.* **2021**, 7.

[4] J. T. Li, M. M. Naiini, S. Vaziri, M. C. Lemme, M. Ostling, *Adv. Funct. Mater.* **2014**, 24, 6524.